Near-Field Scanning Optical Microscopy Studies of Electric-Field-Induced Molecular Reorientation Dynamics

Erwen Mei and Daniel A. Higgins*

Department of Chemistry, Kansas State University, Manhattan, Kansas 66506

Received: March 25, 1998; In Final Form: June 16, 1998

A new form of near-field scanning optical microscopy (NSOM) for studying electric-field-induced dynamics in highly localized regions within birefringent thin film materials is presented. The method is applied to dynamics studies of polymer-dispersed liquid crystal (PDLC) films. A sinusoidally modulated voltage is applied between the NSOM probe and a conductive substrate upon which the PDLC film is supported. A concentrated electric field is formed within the film directly beneath the probe. Time-dependent molecular motion induced by this field is observed via crossed-polarized, transmitted-light near-field optical methods. It is shown that dynamics in volumes as small as 10^{-15} cm^3 may be probed using this method. Via lock-in detection of the optical signal, amplitude and phase images of the local dynamics are recorded. Contrast in these images is utilized to better understand the local-field-induced reorientation process. Information on both the path through which the molecules reorient and spatial variations in the time scale for reorientation is obtained.

I. Introduction

The physical properties of mesostructured thin film materials vary dramatically on micrometer to nanometer distance scales. The need to better understand the local properties of such materials has led to the development of a number of new microscopic methods. Near-field scanning optical microscopy (NSOM) is one such method that simultaneously provides both high-resolution optical and topographic information.[1−4] NSOM has been employed to characterize static molecular organization in a variety of materials via several near-field optical contrast mechanisms.[1,3,5−10] Molecular reorientation processes, whether due to random events or in response to an externally applied perturbation (i.e., an electric field) are also of great importance. Again, for mesostructured materials, reorientation dynamics are expected to vary dramatically as a function of location within individual samples. New NSOM methods are currently being developed for studies of these phenomena. The first observation of random molecular rotational motion by NSOM has just recently been published.[11]

The polymer-dispersed liquid crystal (PDLC) films[12,13] studied here represent a class of materials for which electric-field-induced molecular reorientation phenomena are of great importance. PDLC films are comprised of micrometer-sized and smaller droplets of liquid crystal (LC) dispersed in an otherwise optically uniform polymer film. Their inherent mesostructured nature makes them useful in technologically important optical systems. It is well-known that both their static and dynamic properties vary on submicrometer distance scales. Static molecular organization in PDLCs has been characterized by a number of optical microscopic methods,[12,14−16] including NSOM.[9,10] Although molecular reorientation in thin LC films has been studied in the past by different NSOM methods,[17] LC reorientation dynamics in PDLCs have been probed primarily by bulk optical methods.[18−21] In these studies, uniform electric fields were applied across macroscopic PDLC films, inducing reorientation throughout. The dynamics observed represent an average picture of the LC response in a large number of droplets. As a result, the dynamics were found to be complex, showing multiple time scales for molecular reorientation. This dynamical complexity was attributed to spatial variations in the film properties that could not be resolved by the methods employed.

Here, we present a new near-field optical method that allows for the study of electric-field-induced molecular reorientation dynamics in highly localized regions within PDLC films. For these studies, a sinusoidally modulated voltage is applied between the aluminum-coated NSOM probe and a conductive, optically transparent substrate upon which the sample is supported. A concentrated electric field is formed directly beneath the "sharp" (300 nm end diameter) metallized probe. The induced time-dependent motion of the molecules is observed via resulting time-dependent variations in the local optical properties of the sample. These properties are probed by detecting the light transmitted through the birefringent LC droplets under crossed-polarization conditions. Lock-in detection of the optical signal provides amplitude and phase data for the recording of dynamic NSOM images. The use of near-field optical methods for observation of the dynamics further confines the volume in which the dynamics are probed.

II. Experimental Considerations

The near-field microscope employed has been described previously.[10] Briefly, topographic imaging and tip−sample distance regulation were performed by well-known shear-force feedback methods.[22,23] Aluminum-coated NSOM probes with ∼125 nm diameter apertures (determined by SEM) were produced in-house. SEM images of the probes showed the Al coating to be smooth (i.e., free of Al aggregates, needles, and pits) down to less than 20 nm dimensions (the approximate resolution of the SEM).

For optical imaging, the 514 nm line of an argon ion laser was passed through $\lambda/2$ and $\lambda/4$ plates to control the polarization

* Corresponding author.

S1089-5639(98)01633-8 CCC: $15.00
Published on Web 09/09/1998

of light from the NSOM probe. Optical images were recorded in the transmitted-light mode using a 60×, 0.7 numerical aperture objective to collect light coupled through the sample. An analyzer ($>10^5$ extinction) was fixed in the output path and was oriented perpendicular to the incident polarization. Polarization purity under such conditions was always observed to be >99%. Detection of the transmitted light was accomplished using a conventional photomultiplier tube (PMT).

For dynamics studies, thin copper wires (125 μm diameter) were attached to the probe and substrate. The probe wire was attached ~3 mm above the probe tip. The presence of the wire did not adversely affect tip−sample distance regulation. The internal oscillator of a lock-in amplifier was used to generate the sinusoidally modulated voltage (symmetric about 0 V). Dynamics data have been recorded using modulation frequencies ranging from 100 to 3000 Hz; however, all data presented here were recorded at 200 or 300 Hz. For optical detection of LC dynamics, the output of the PMT, taken across a 1000 Ω load, was fed into the voltage input of the lock-in amplifier. The amplitude and phase signals from the lock-in, recorded at the second harmonic of the driving field (see below), were acquired for imaging purposes. Dynamics images of the droplets recorded using different NSOM probes did not show significant differences.

The polymer encapsulation method was used to prepare the PDLC films.[24] A 0.67% (by weight) emulsion of nematic LC (E7, Merck) in a 2% (by weight) aqueous solution of poly(vinyl alcohol) (PVA) was first prepared. Thin films were formed by depositing a few drops of the emulsion onto an indium tin oxide (ITO) coated glass substrate and allowing the water to evaporate. The LC droplets formed ranged from about 1−20 μm in diameter. It has been shown that these droplets are encapsulated in a relatively solid PVA shell of less than 20−40 nm thickness and are dispersed in a surrounding polymer film of ~1 μm thickness.[10] From static optical and topographic images, the droplets formed may be characterized as being of spheroidal, discoidal, or toroidal shape.[10]

III. Results and Discussion

The optical signal in dynamics experiments results from the field-dependent reorientation of the LC molecules beneath the probe. In most cases, the molecules reorient from a zero-field state, in which their long axes (nematic directors) are aligned approximately parallel to the film surface, to one in which they are aligned normal to the surface. Thus, reorientation leads to a change in the extent to which local regions in the birefringent LC droplets alter the polarization of transmitted light.

Detected under crossed-polarized conditions, the resulting optical signal is expected to be a complex function of the time-dependent electric field. A representative signal trace is shown in Figure 1. Under the specific conditions employed, the signal appears as a sine wave (to a good approximation) at the second harmonic of the driving field. Appearance of the signal at the second harmonic is expected. LC alignment is essentially independent of the sign (direction) of the field. In addition, the optical properties of the LC are independent of absolute molecular direction (static dipole parallel or antiparallel to the field). However, the apparent simplicity of the optical response cannot be predicted a priori. In fact, the waveform is observed to become distinctly nonsinusoidal in some frequency and voltage ranges (see below). For all imaging experiments described below, the modulation parameters employed resulted in sinusoidal signal waveforms.

Part of the complexity in the optical signal is due to the strong field and frequency dependence of the molecular reorientation process. At low fields, a distinct threshold is observed below which little or no reorientation occurs. As has been shown in bulk experiments[12,13,18,20,25] and as is observed in the present studies, approximately 1 V/μm is required to induce molecular motion (known as the Frederiks transition).[26] This threshold corresponds to the field needed to overcome the intermolecular (LC−LC and polymer−LC) forces holding the molecules in their original configuration.[18,19] At higher fields, depending on the modulation frequency (~6 V/μm at 200−300 Hz), the optical signal is observed to saturate. Saturation occurs when all molecules beneath the probe are completely reoriented by the field. In cases of severe saturation, the signal no longer approximates a sine wave.

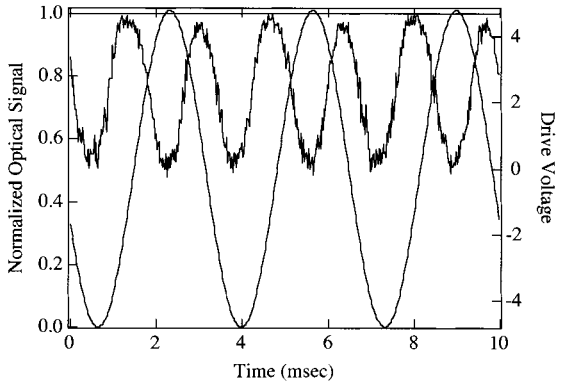

Figure 1. Plot of the voltage applied between tip and sample at a frequency of 300 Hz. Also shown is the optical signal detected with the NSOM probe positioned over a single LC droplet. The data were recorded under crossed-polarization conditions using a digital oscilloscope. The dynamic signal is an average of 16 oscilloscope traces and is normalized to the static (zero field) signal observed in this region.

The signal also varies dramatically with modulation frequency. These variations are mostly restricted to monotonic changes in the amplitude (decreases with increasing frequency) and phase (recedes with increasing frequency) and are due to the finite reorientation time of the LC molecules (typically a few milliseconds).[18] Time- or frequency-dependent studies may therefore be useful as a means to quantitatively measure the local reorientation rate in the future.[27] However, other factors cause the signal to vary with frequency as well, including the frequency-dependent dielectric properties of the surrounding polymer matrix.[28]

The hypothesis that only a small volume of LC is reoriented using the present methods may be addressed from both theoretical and experimental perspectives. In qualitative terms, it is well-known that a potential applied to a "sharp" metallic probe produces a concentrated field at the end of the probe. More quantitative support for such a conclusion is obtained from results of model calculations, as shown in Figure 2. These calculations also provide a means to estimate the volume in which LC reorientation is directly induced. For this simulation, Laplace's equation was solved numerically in two dimensions for a 4 V potential applied between tip and substrate. The two were taken to be separated by a 1 μm thick, uniform, isotropic, dielectric medium. In Figure 2, the field strength is greatest (~10 V/μm) at a few nanometers from the end of the probe and falls rapidly to 50% of this value within a distance of 200 nm.

Although all fields shown in Figure 2 are above threshold (~1 V/μm), in actual experiments, the fields will be much smaller. In the real system, the tip and substrate are presumed to be separated by a small (~5−10 nm thick) air gap or surface contamination layer on top of the ~1 μm thick polymer film.

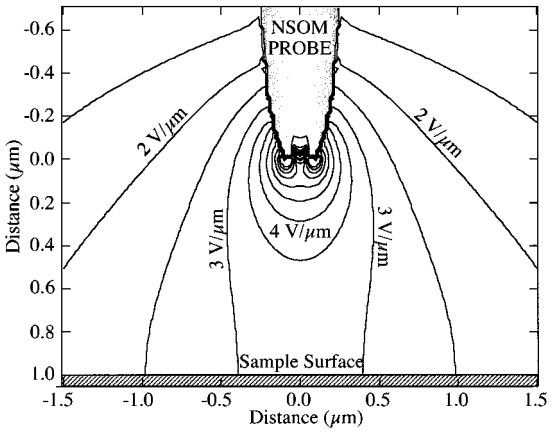

Figure 2. Contour lines of constant electric field strength between NSOM probe and conducting substrate. A uniform, isotropic dielectric medium is assumed to separate the two. The results were obtained by numerically solving Laplace's equation in two dimensions. Field strengths up to 7 V/μm are shown.

The dielectric constant of PVA is ~11 at 1 kHz.[28] Although difficult to model exactly, it is expected that the fields will therefore fall below threshold at distances of greater than a few hundred nanometers. The volume of LC directly reoriented by the field may then be as small as 10^{-14} cm^3 for small (~4 V) applied potentials.

The above conclusions are supported by the data presented in Figure 1. Although strong modulation is observed in the signal, the fact that the modulation depth is much less than 100% indicates that only a fraction of the LC molecules beneath the probe are being reoriented. Were all such molecules to align normal to the film surface, the birefringent LC would no longer alter the polarization of the transmitted light. Under crossed-polarization conditions, the signal would then go to zero near the peak of the modulated field (see Figure 1). The reduced modulation depth observed may result from the finite reorientation time of the LC, prohibiting large-amplitude molecular motions. However, at the low modulation frequency employed (300 Hz), this effect should be minimized (but not necessarily negligible). The proposal that the applied fields only reorient a small volume of the LC beneath the probe represents an alternative explanation. Confinement of the reoriented volume will effectively reduce the depth of modulation, as observed in Figure 1. Both effects likely contribute to some degree.

By optically detecting LC motion via near-field methods, the lateral dimension over which such motion is observed is further confined to a cross-sectional area determined by the size of the NSOM probe aperture (~125 nm for our probes). The near-field regime is confined to a distance of ~125 nm from the end of the probe. Since these samples are relatively thick (~1 μm), much of the volume probed may be in the far field. In this case, the light will have spread laterally so that the cross-sectional area is no longer limited by the probe size. The actual volume in which the dynamics are observed is represented by the mathematical intersection of the volume in which switching is induced and the total volume (including both near-field and far-field regions) through which the transmitted light passes. However, with careful selection of the switching voltage, it can be concluded that the volume probed may be as small as 10^{-15} cm^3 in some cases but in fact may be larger and more on the order of 10^{-14} cm^3 for cases in which much of the sample is in the far field.

Regardless of the above limitations, dynamics images obtained via lock-in detection of the modulated optical signal provide a valuable new means for spatially resolving variations in the reorientation dynamics. Figures 3 and 4 show topographic and dynamic (amplitude and phase) optical images of two representative droplets. The amplitude images are nearly identical to static (zero field) optical images of the same droplets, acquired by simply recording the transmitted light intensity under crossed-polarization conditions.[10] However, the optical signal shown here results solely from the molecular reorientation process. Conclusive proof is shown in the line scans presented in Figure 3. The signal from approximately the same line scan in two different images of the same droplet, recorded at potentials of 4 V_{rms} and 0 V, are shown. The insignificant contrast observed at 0 V is due to imperfect rejection of the static signal component by the lock-in amplifier under the experimental conditions employed (200 Hz fundamental frequency, 50 Hz detection bandwidth).

The data presented in Figure 1 provide a means for gauging the optical contrast in Figures 3 and 4. As noted previously,[10] the maximum static optical signal observed (corresponding approximately to the peak in the modulation signal at low frequencies) approaches that expected for 90° polarization rotation by the birefringent LC droplets. The difference between the LC extraordinary and ordinary refractive indices, $\Delta\eta$, is ~0.22 at the wavelength employed, and the film thickness is ~1 μm. The fact that close to 90° polarization rotation is observed in some cases implies that passage of the light through the far-field region of the sample significantly alters the optical signal. However, as shown in Figure 1, at low frequencies and low field strengths, the maximum depth of modulation is typically much less than 100% of the static signal and is usually in the 30−50% range. As discussed above, the reduced modulation depth suggests that only a small volume of LC near the top of the droplet is being reoriented. Again, since the dynamic signal only arises from field-induced changes in the LC orientation, the depth to which the properties of the LC droplet are probed is expected to be much more confined. Hence, contributions from far-field effects should be greatly reduced in the dynamics images.

The similarity between the static and dynamic (amplitude) images provides important information on the reorientation process. In particular, contrast in the amplitude images is determined in part by the angular path through which the LC directors rotate during electric-field-induced reorientation. To interpret the images, the static (or relaxed) LC organization must first be determined, as has been done previously.[10] From these results, it is concluded that the droplet shown in Figure 3 is a toroidally shaped droplet with the encapsulated LC organized in a toroidal configuration. The model presented in Figure 3D shows the approximate zero-field director organization within this droplet. In contrast, the droplet shown in Figure 4 is of a spheroidal shape and the LC is organized in the well-known "bipolar configuration".[29] A model for the LC organization within this droplet is shown in Figure 4D. For this droplet, an optical axis (the average director direction) may be defined. The optical axis is aligned in the plane of the film and rotated ~25° clockwise from horizontal (on the image).

Contrast in static optical images results solely from variations in the extent to which the polarization of the transmitted light is altered by the birefringent droplet. In the dynamic images, the same birefringence effects now provide time-dependent optical contrast related to the time-dependent motion of the LC molecules. As with the static images, the dark and light regions in the amplitude images tell how the local directors are aligned

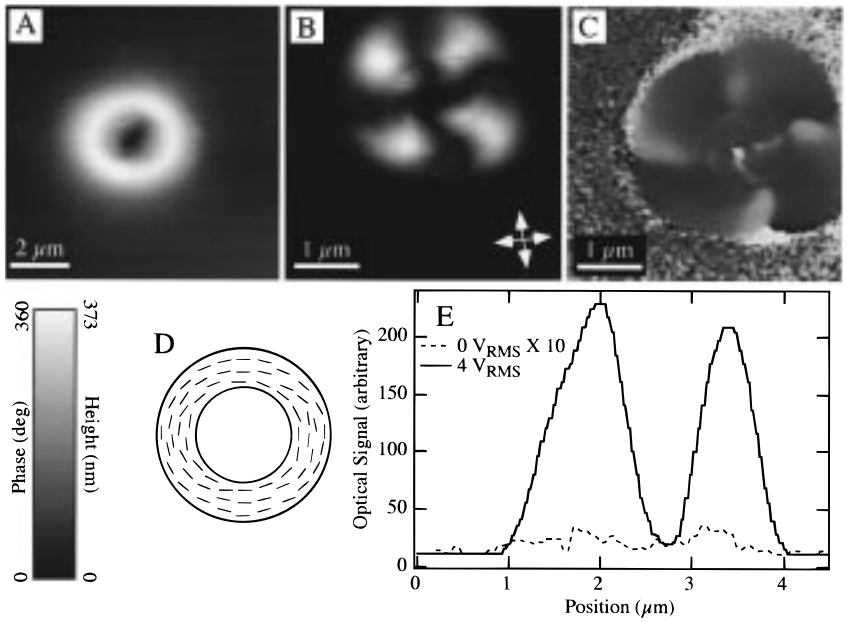

Figure 3. (A) Topographic image of a toroidal droplet and (B) amplitude and (C) phase images acquired by recording the dynamic optical signal for the same droplet. The voltage applied between tip and sample was modulated at 200 Hz and had a 4 V_{rms} amplitude. The alignments of input and output polarizations are shown (input is approximately horizontal; output is approximately vertical) in (B). (D) Organization of the LC molecules within this droplet in the relaxed, zero-field state, as determined in static imaging experiments.[10] The long molecular axis, or director, (represented by the short lines in (D)) of each molecule lies in the plane of the film. (E) Line scan across the amplitude image shown in (B) at 4 V_{rms} and 0 V (10× scale). These data demonstrate that the signal observed in (B) and (C) results solely from LC reorientation.

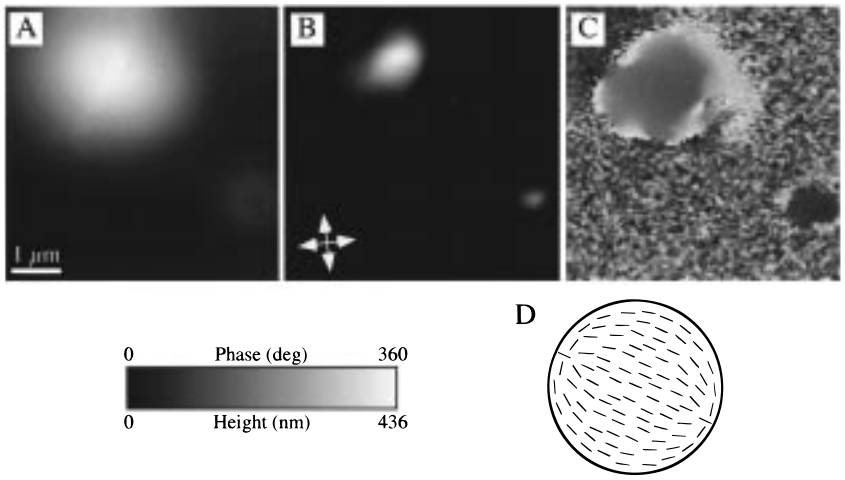

Figure 4. (A) Topographic image of a spheroidal droplet and (B) amplitude and (C) phase images acquired by recording the dynamic optical signal for the same droplet. The voltage applied between tip and sample was modulated at 200 Hz and had a 4 V_{rms} amplitude. The alignment of the input and output polarizations are shown (input is approximately horizontal; output is approximately vertical) in (B). (D) Model for the well-known "bipolar configuration" for the LC organization within this droplet.[29] The optical axis of the droplet (the average orientation of the molecular directors) is oriented approximately in the plane of the sample and rotated ∼25° clockwise from horizontal.

with respect to the incident and detected polarization axes, throughout the reorientation process. In the dark regions, projections of the directors in the sample plane remain aligned parallel or perpendicular to either the incident or detected polarization axes throughout reorientation. In the bright regions, the director projections are rotated off the polarization axes. The strong contrast observed in the amplitude image shown in Figure 3 therefore indicates that the directors must reorient along a trajectory that allows their projections to remain fixed in the sample plane. That is, the long axes of the molecules must reorient in a plane defined by the applied field and the local static (zero field) director orientation. Were the molecules to rotate (possibly in a spiral motion) out of this plane, a strongly modulated optical signal would be observed in all regions of the droplet. If this were the dominant motion, the amplitude images would appear uniformly bright. Spatial variations in the optical signal would then primarily appear in the phase data (see below). Although this type of motion is not expected in most cases, it is possible that it could be induced in droplets of certain distorted shapes.

Although qualitative information on the reorientation process is obtained from the amplitude images, quantitative data on variations in the reorientation rate cannot be obtained for two reasons. First, as described above, the amplitude images are highly dependent on local LC orientation. Second, the amplitude signal is also dependent on the amount of birefringent material present beneath the probe (i.e., the thickness of the sample probed).

The phase data are much less sensitive to such effects. Therefore, the phase images shown in Figures 3 and 4 present a potentially better means for observing spatial variations in the reorientation rate. As the modulation frequency approaches the local reorientation rate, the phase of the modulated optical signal will recede. For the majority of regions within the droplets, the lock-in amplifier reports a phase angle near 90° (see Figures 1, 3, and 4) for low modulation frequencies. The optical signal (second harmonic) has a minimum when the modulated field is near its peak. As observed in Figure 4 (spheroidal droplet), the measured phase angle increases near the droplet edge, indicating that the dynamics are different in the center of the droplet than they are near the polymer−LC interface. Previously published bulk studies have proposed that the reorientation dynamics near the polymer−LC interface should be slower than in central regions for spheroidal droplets.[18] This phenomenon has been attributed to strong polymer−LC interfacial interactions that tend to hold the molecules in their original orientation. However, the increase in phase angle observed in the edge region implies that the dynamics are faster in this region than they are in the center of the droplet. Were the dynamics slower, the phase angle would recede (i.e., shift toward negative angles) rather than increase. Recent experiments in which the local reorientation rate was directly measured prove that the dynamics are indeed faster in the edge region.[27]

Although the phase data near the droplet edge appear to contradict previously published models, this discrepancy may simply result from differences in the experimental methods employed. The previously published work attributed dynamics occurring on the 10−100 ms time scale to interfacial LC reorientation. Again, these observations were made following field-induced reorientation of the entire PDLC sample under the influence of a uniform electric field. In contrast, only a small volume of the LC is reoriented in the present experiments. Also, the dynamics that are observed here occur primarily on the submillisecond time scale. Therefore, it is likely that the dynamics observed in the edge regions are due to different phenomena. The faster dynamics observed near the edges are likely due to reorientation of the LC in layers adjacent to those at the interface. As has been suggested previously, reorientation of the molecules right at the interface may be too slow to observe here.[18]

A new model for the dynamics may therefore be developed on the basis of this new information. The LC configuration in the field-off state is determined primarily by minimization of bend and splay deformations.[16] Under the influence of an applied field, a balance is achieved between the field effects and these deformations. Near the center of the droplet, the LC molecules may simultaneously align parallel to the applied field and parallel to each other. When the field is removed, the LC molecules remain parallel to each other. Relaxation likely occurs by collective rotation of the LC directors back to their relaxed state. Previous studies have proposed that this is a slow process.[18] Near the polymer−LC interface, the director field is highly curved (see Figure 4D) in the zero-field state. Individual LC molecules cannot align strictly parallel to their neighbors. Their alignment with respect to each other, on a local scale, under the influence of the applied field will be different from this relaxed state. Once the field is removed, these molecules will then rapidly relax to minimize bend and splay deformation. The overall LC organization, however, may still appear similar to that observed under the influence of the applied field. Complete relaxation may take much longer, perhaps 10−100 ms.[18,27] Given such a model, the dynamics would most certainly be observed to be faster near the polymer−LC interface than they are in the center of the droplet.

Variations observed in the phase angle around the droplet circumference (see Figure 4) are due to the presence of defects in the LC organization. In fact, for a perfect bipolar configuration (see Figure 4), two such defects are expected.[29] The phase angle measured in these areas again indicates that the dynamics are slower than in the neighboring edge regions. The differences may be explained with arguments similar to those given above. The LC directors are significantly disordered in these regions in the zero-field state; therefore, alignment parallel to the field produces a more energetically favorable state (locally). This model suggests that only a small driving force for return to their original state exists, and hence, the dynamics are expected to be slower.

In contrast to the dramatic edge effects observed for the spheroidal droplet, only weak effects are observed in the phase image of the toroidal droplet (see Figure 3). Although this observation may appear to contradict the results for the spheroidal droplet, it may be explained with the same arguments presented above. It is also supported by the conclusions of previous bulk studies.[18] The toroidal droplet shape will yield a much deeper energy minimum for the relaxed organization throughout the droplet. Therefore, the driving force for relaxation in this "highly shaped" droplet will be much greater throughout and also will be more "uniform". This expectation is again consistent with the contrast observed in the phase image.

The four-lobed pattern observed in the phase image for the toroidal droplet (Figure 3) is not due to lateral variations in the dynamics within the droplet. This effect may be explained by variations in the optical contrast mechanism. Such variations are proposed here to provide information on the depth dependence of the dynamics. The possibility of lateral variations in the dynamics is discounted by recording multiple images using several alignments of the input and output polarizers (while maintaining their orthogonal relationship). In these experiments, the optical pattern simply rotates with the polarization axes.

The contrast mechanism in the phase image likely varies from one based solely on conventional polarization phenomena to one involving a complex near-field phenomenon. The intensity of light coupled from the near field to the far field is known to be highly dependent on the refractive index of the medium directly beneath the probe.[30] As the refractive index increases, so does the intensity of light coupled to the far field. In regions where the conventional contrast mechanism is no longer important, the effects of this near-field phenomenon become readily apparent.

The dark regions in the amplitude image shown in Figure 3 are regions where the LC directors are aligned parallel or perpendicular to the polarization axes. Hence, in these regions, the polarization of transmitted light passes unaltered. However, the amplitude signal in these regions is not exactly zero but is 5−10% of the average signal observed in the bright regions. Exactly the same regions in the phase image show a dramatic ∼180° phase shift from that observed for the surrounding bright regions. The dynamic optical signal in these regions likely comes from the near-field effect described above. The polarization of light from the NSOM probe is imperfect and includes a significant nonzero component polarized normal to the sample plane.[31] This component is not totally blocked by the analyzer, since the objective lens converts it to a distribution of polarizations in the analyzer plane. As the molecules align parallel to the field, this component of the optical field (in the near-field regime) experiences the much greater extraordinary refractive

index of the LC, increasing its coupling to the far field. As the applied electric field reaches its peak, the optical signal should also reach its maximum value. Note that this suggests a 180° phase shift from the surrounding regions, as is observed. Because the signal results from a near-field effect, it may be attributed to reorientation of the molecules nearest the upper polymer−LC interface.

A few caveats to the above interpretations must be mentioned. Most notably, the electric field does not remain constant as the probe is scanned across the droplet. The field strength is largest near the edge region, suggesting that an increase in the LC response rate near the edge might be expected. However, it is the rate at which the molecules relax (as the field decreases) that dominates the dynamics. This rate is essentially independent of field strength. The field direction does, however, vary in a complex fashion within the droplet as edges or defects are approached. Such variations are difficult to predict without extensive modeling and detailed information on droplet shape and physical properties. Therefore, directional variations in the field cannot be readily discounted as a possible contrast mechanism in the above images. Finally, as described above, the contrast mechanism may vary depending on the detailed molecular alignment in relation to the polarization axes. Incorporation of the near-field polarization effect to varying degrees may lead to significant optical contrast in both spheroidal and toroidal droplet images. Detailed studies of the contrast mechanism are underway to conclusively determine the source of the contrast. Finally, as noted, future experiments will use measurements of the local time- or frequency-dependent response of the molecules to unambiguously determine the time scale for electric-field-induced reorientation in local sample regions.

IV. Conclusions

A new optical microscopic method for studying electric-field-induced molecular reorientation dynamics in mesostructured materials has been presented. Based on near-field scanning optical microscopy, this method allows for studies of dynamics in sample volumes that may be as small as 10^{-15} cm^3. Dynamic optical images of polymer-dispersed liquid crystal films were acquired. Contrast observed in the images was attributed in part to spatial variations in the dynamic response of the LC molecules to an applied field. The images were also employed to better understand the reorientation process within the PDLC films.

Acknowledgment. This work was supported in part by the National Science Foundation through the CAREER Award program (CHE-9701509) and through an NSF Special projects grant (CHE-9617774). Kansas State University is also acknowledged for its support of this work. Xiangmin Liao is acknowledged for characterization of the NSOM probes by SEM.

References and Notes

(1) Vanden Bout, D. A.; Kerimo, J.; Higgins, D. A.; Barbara, P. F. *Acc. Chem. Res.* **1997**, *30*, 204.
(2) Betzig, E.; Trautman, J. K.; Harris, T. D.; Weiner, J. S.; Kostelak, R. L. *Science* **1991**, *251*, 1468.
(3) Betzig, E.; Trautman, J. K.; Weiner, J. S.; Harris, T. D.; Wolfe, R. *Appl. Opt.* **1992**, *31*, 4563.
(4) Dürig, U.; Pohl, D. W.; Rohner, F. *J. Appl. Phys.* **1986**, *59*, 3318.
(5) Higgins, D. A.; Reid, P. J.; Barbara, P. F. *J. Phys. Chem.* **1996**, *100*, 1174.
(6) Higgins, D. A.; Kerimo, J.; Vanden Bout, D. A.; Barbara, P. F. *J. Am. Chem. Soc.* **1996**, *118*, 4049.
(7) Higgins, D. A.; Vanden Bout, D. A.; Kerimo, J.; Barbara, P. F. *J. Phys. Chem.* **1996**, *100*, 13794.
(8) Betzig, E.; Chichester, R. J. *Science* **1993**, *262*, 1422.
(9) Ade, H.; Toledo-Crow, R.; Vaez-Iravani, M.; Spontak, R. J. *Langmuir* **1996**, *12*, 231.
(10) Mei, E.; Higgins, D. A. *Langmuir* **1998**, *14*, 1945.
(11) Ruiter, A. G. T.; Veerman, J. A.; Garcia-Parajo, M. F.; van Hulst, N. F. *J. Phys. Chem. A* **1997**, *101*, 7318.
(12) Drzaic, P. S. *J. Appl. Phys.* **1986**, *60*, 2142.
(13) Doane, J. W.; Vaz, N. A.; Wu, B.-G.; Zumer, S. *Appl. Phys. Lett.* **1986**, *48*, 269.
(14) Drzaic, P. S. *Mol. Cryst. Liq. Cryst.* **1988**, *154*, 289.
(15) Ondris-Crawford, R.; Boyko, E. P.; Wagner, B. G.; Erdmann, J. H.; Zumer, S.; Doane, J. W. *J. Appl. Phys.* **1991**, *69*, 6380.
(16) Kitzerow, H.-S. *Liq. Cryst.* **1994**, *16*, 1.
(17) Moyer, P. J.; Walzer, K.; Hietschold, M. *Appl. Phys. Lett.* **1995**, *67*, 2129.
(18) Drzaic, P. S. *Liq. Cryst.* **1988**, *3*, 1543.
(19) Erdmann, J.; Doane, J. W.; Zumer, S.; Chidichimo, G. *Proc. SPIE* **1989**, *1080*, 32.
(20) Jain, S. C.; Rout, D. K. *J. Appl. Phys.* **1991**, *70*, 6988.
(21) Jain, S. C.; Thakur, R. S.; Lakshmikumar, S. T. *J. Appl. Phys.* **1993**, *73*, 3744.
(22) Betzig, E.; Finn, P. L.; Weiner, J. S. *Appl. Phys. Lett.* **1992**, *60*, 2484.
(23) Toledo-Crow, R.; Yang, P. C.; Chen, Y.; Vaez-Iravani, M. *Appl. Phys. Lett.* **1992**, *60*, 2957.
(24) Doane, W. J. Polymer Dispersed Liquid Crystal Displays. In *Liquid Crystals: Applications and Uses*; Bahadur, B., Ed.; World Scientific: Singapore, 1990; Vol. 1, p 361.
(25) Lin, H.; Ding, H.; Kelly, J. R. *Mol. Cryst. Liq. Cryst.* **1995**, *262*, 99.
(26) De Gennes, P. G.; Prost, J. *The Physics of Liquid Crystals*, 2nd ed.; Oxford University Press: New York, 1993.
(27) Mei, E.; Higgins, D. A. *Appl. Phys. Lett.*, submitted.
(28) Ishida, Y.; Takada, Y.; Takayanagi, M. *Kolloid Z.* **1960**, *168*, 121.
(29) Zumer, S.; Doane, J. W. *Phys. Rev. A* **1986**, *34*, 3373.
(30) Novotny, L.; Pohl, D. W.; Regli, P. *J. Opt. Soc. Am. A* **1994**, *11*, 1768.
(31) Bouwkamp, C. J. *Philips Res. Rep.* **1950**, *5*, 321.